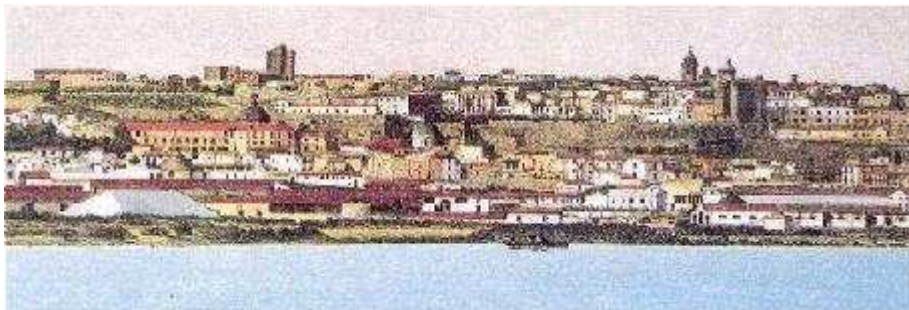


**Università degli Studi di Cagliari**  
**Facoltà di Ingegneria**  
Dipartimento di Ingegneria Meccanica

**5<sup>TH</sup> SEMINAR ON  
EXPERIMENTAL TECHNIQUES AND DESIGN  
IN COMPOSITE MATERIALS**

**Sant'Elmo Beach Hotel**  
**Costa Rei (Cagliari), Italy**  
September 28-29, 2000



## **ORGANIZED BY**

Università di Cagliari

Dipartimento di Ingegneria Meccanica

## **SPONSORS**

Regione Sardegna

Assessorato degli Affari Generali, Personale e Riforma della Regione

Camera di Commercio di Cagliari

Saras S.p.A.

## **SCIENTIFIC COMMITTEE**

P. Priolo, *University of Cagliari, Italy*

B. Atzori, *University of Cagliari, Italy*

P.W.R. Beaumont, *University of Cambridge, UK*

M.S. Found, *University of Sheffield, UK*

F. Ginesu, *University of Cagliari, Italy*

R. Talreja, *Georgia Tech, USA*

## An Elastic-Interface Model for Delamination Buckling in Laminated Plates

Stefano Bennati and Paolo S. Valvo

University of Pisa – Department of Structural Engineering  
Via Diotisalvi, 2 – I 56126 PISA – Italy  
e-mail: [s.bennati@ing.unipi.it](mailto:s.bennati@ing.unipi.it), [p.valvo@ing.unipi.it](mailto:p.valvo@ing.unipi.it)

**Keywords:** delamination buckling, laminated plate, elastic interface, mixed-mode crack-growth.

**Abstract.** This paper presents a one-dimensional model of a composite laminated plate containing a delamination and subject to uniaxial compression, where the delaminated plate is thought of as two sublaminates partly connected by an elastic interface. This is a continuous distribution of normal and tangential linear elastic springs, aiming to model the behavior of the thin layer of resin joining the laminae together in a real laminate. The nonlinear equilibrium equations, derived from von Kármán's plate theory, are solved explicitly and the normal and tangential interlaminar stresses are determined. The virtual crack closure technique is used to deduce the expressions of the mode-I and mode-II energy release rates, needed for applying a mixed-mode crack-growth criterion.

### Introduction

Composite laminated plates are successfully used in many structural applications, thanks to their high strength and stiffness compared to their low specific weight. Unfortunately, these materials are also very sensitive to damage and their attractive properties suffer the presence of defects, such as interlaminar cracks or delaminations, frequently due to manufacturing errors or produced during service (e.g. by low-velocity impacts). Whatever might be their origin, delaminations can drastically reduce the stiffness and the load-carrying capacity of a structure.

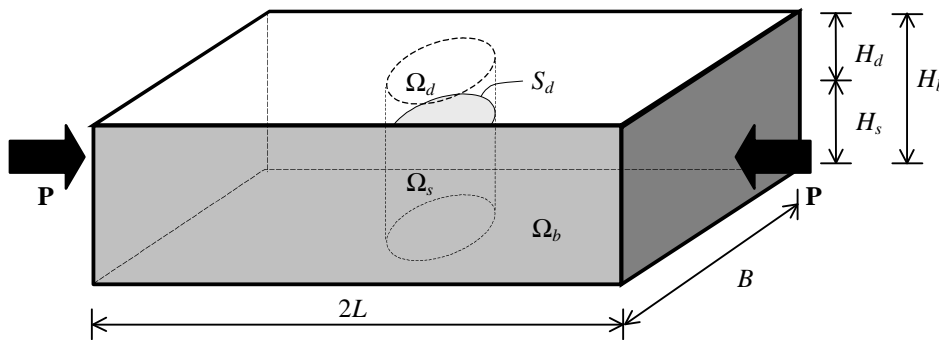


Figure 1 – Delaminated plate loaded in compression.

Consider a laminated plate containing a delaminated surface, or delamination,  $S_d$ , generic in shape and location, parallel to the middle plane of the plate (Fig. 1). Three different regions can be defined in the plate: the delaminated region,  $\Omega_d$ , included between the delamination and the nearest external surface; the substrate,  $\Omega_s$ , between the delamination and the farthest surface; and, finally, the base laminate,  $\Omega_b$ , unaffected by the presence of the delamination. Under compressive loads, complex instability phenomena can occur, involving both the global buckling of the whole plate and the local buckling of the regions  $\Omega_d$  and  $\Omega_s$ . Furthermore, in the post-critical phase, high interlaminar stresses arise in the neighborhood of the delamination front,  $\partial S_d$ , thus promoting crack growth. As the delamination becomes larger, the geometry of the delaminated plate changes and, in general, a new equilibrium state is found. The process may lead to stable growth and crack arrest or to unstable growth until final failure.

Literature on delamination buckling is very extensive and a complete account cannot be given here. The first studies on the subject were by Kachanov [1] and Chai *et al.* [2], who introduced the *Thin Film Model (TFM)* and the *Thick Column Model (TCM)*. Other pioneering contributions were given by Whitcomb [3], Bottega and Maewal [4] and Yin [5]. Afterwards, many theoretical and experimental studies have been carried out. A number of cases have been analyzed, differing for the geometry and the boundary conditions of the plate, for the number, the shape and the position of the delaminations. Many solution strategies have been proposed, both analytical and numerical. Despite this great effort of research during the last two decades, a complete understanding of the phenomenon is far from being reached. Delamination buckling is still a topic of research and many questions, such as anisotropy [6], interface modeling [7], fiber bridging [8], crack nucleation [9], mixed-mode crack-growth and so on, deserve a deeper investigation. Also computational techniques need to be refined [10] and a continuous comparison with experimental results is necessary [11].

In the delamination buckling process, the phenomena of instability and fracture are intimately related and take place simultaneously. Actually, some studies [4,12] have proposed a variational formulation to derive both the equilibrium solution and the crack growth from a unique suitably defined functional. However, the prevailing approach is to analyze the two aspects separately: firstly, the nonlinear equilibrium problem is solved and secondly a crack-growth criterion is applied.

The stability problem can be dealt with in the framework of elasticity theory [13]. This approach has the advantage that interlaminar stresses, responsible for crack growth, are obtained as a part of the solution. On the other hand, considerable analytical difficulties must be faced, even having recourse to numerical methods. Therefore, most studies are based on the structural theories [14]. The delaminated plate is then modeled as an assemblage of beams and plates, but any *direct* information about interlaminar stresses is lost.

As far as the fracture phenomenon is concerned, the classical tools of fracture mechanics are usually employed. *Local* parameters describing the singular stress-field at the delamination front, such as the stress-intensity factors,  $k_I$ ,  $k_{II}$ , and  $k_{III}$ , are obtained directly when the post-critical solution is found via elasticity theory [15]. Instead, when a structural model is used, they can be estimated *a posteriori* from the computed solution [16]. Alternatively, a *global* parameter, such as the energy release rate,  $G$ , can be considered. An advantage in doing this is that many methods exist to evaluate  $G$  rather easily (e.g. by numerical differentiation, by invariant integrals, etc.) [17], while a considerable drawback is that no distinction among the three different modes of crack growth (opening, sliding, and tearing) is usually possible. Instead, experimental studies have repeatedly highlighted the need of a mixed-mode crack-growth criterion in the case of composite laminates, where fracture toughness is much greater in mode II (sliding) than in mode I (opening) [18].

A more detailed description of the process of layer separation can be achieved by the theory of interface models. In this case, the laminated plate is schematized as a stacking of laminae, bonded together by interposed interface layers of zero thickness [19]. Interlaminar stresses are modeled by suitable constitutive laws, which can include the effects of anisotropy, plasticity, viscosity, damage and so on. As the complexity of the interface model grows, however, also difficulties in its use and in the identification of all the necessary parameters increase [20].

The simpler conceivable interface is probably one constituted by a continuous distribution of linear elastic springs. Different values of the elastic constants for the normal and tangential directions can be assumed and a fracture criterion can be introduced by setting an upper limit to the values of the elastic reactions. Models endowed with elastic interfaces have already been proposed for the study of delamination buckling. Vizzini e Lagace first modeled a “delaminated sublaminate” as a beam on an elastic foundation. They considered only normal springs and confined their analysis to the determination of the buckling load [21]. Bruno and Grimaldi analyzed also the post-critical behavior and considered delamination growth by assuming a limit elongation for the springs [22]. Elastic springs also in the tangential direction were considered in some papers [23,24,25], but in

none of these, the normal and tangential interlaminar stresses were computed in view of the application of a mixed-mode crack-growth criterion. Actually, the elastic interface was introduced there to describe the boundary conditions of the delaminated region more accurately than the *TC Model*, which assumed clamped ends. The final aim was a better evaluation of the buckling load, rather than the gain of information on interlaminar stresses.

The present paper describes a one-dimensional model of a laminated plate, containing a through-the-width delamination, subject to uniaxial compression. This *Elastic-Interface Model (EIM)* is constituted by a thinner sublaminar (the so-called film) connected to a thicker one (the substrate) by a continuous distribution of normal and tangential elastic springs. Their elastic constants,  $k_z$  and  $k_x$ , should be chosen in order to reproduce the behavior of the thin layer of resin joining the laminae together in a real laminate [26]. The simplifying “thick column” hypothesis is supposed to hold, so that in the post-critical phase the film undergoes transverse displacements, but not the substrate.

The equations derived from von Kármán’s plate theory, together with the appropriate boundary conditions, lead to a nonlinear differential problem. In the simpler case with no tangential springs ( $k_x = 0$ ), an exact explicit solution is determined, leading to a model called in the following *Winkler-Interface Model (WIM)*, because the interface acts as a Winkler-type foundation. In the general case with both normal and tangential springs ( $k_z \neq 0$  and  $k_x \neq 0$ ), an approximate explicit solution is found. Normal and tangential interlaminar stresses are determined and the virtual crack closure technique is used to deduce the expressions of the mode-I and mode-II energy release rates.

Analytical details cannot be given here for reasons of brevity and will be reported in a forthcoming paper. However, some results in the shape of graphs are presented to highlight the influence that the geometric and elastic parameters have on the structural response. A first comparison among the *EI*, the *WI* and the *TC Models* is made.

### Position of the problem

**The model.** Consider a rectangular plate of length  $2L$ , width  $B$ , and thickness  $H_b$  (Fig. 2). A central through-the-width delamination of initial length  $2a$  is present, at a depth  $H_d$  from the nearest external surface. A rectangular reference system,  $OXYZ$ , is fixed with the origin in the center of the plate and with the axes parallel to its edges. The material is homogeneous and linearly elastic, with orthotropy axes aligned with those of the fixed reference. Let  $E_x, E_y, E_z, G_{xy}, G_{yz}, G_{zx}, \nu_{xy}, \nu_{yz},$  and  $\nu_{zx}$  be its elasticity moduli. Two compressive forces of intensity  $P$  act in the  $X$ -direction.

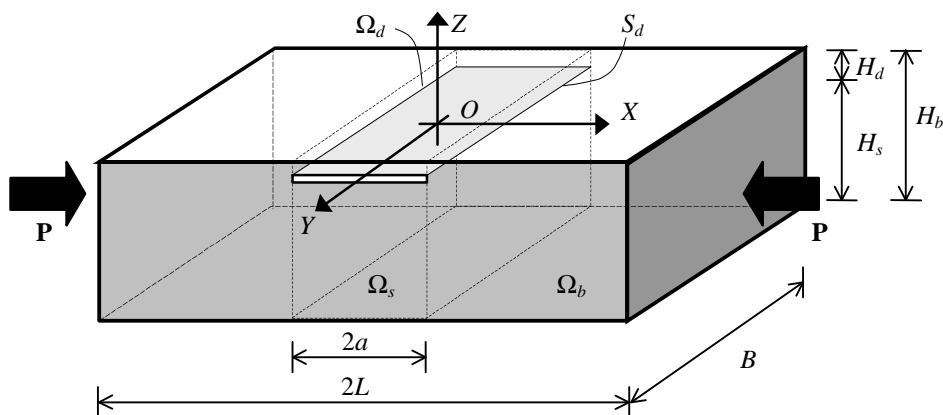


Figure 2 – Plate with a through-the-width delamination, loaded in compression.

Under the above hypotheses, the solution does not depend upon the  $Y$ -coordinate and the delaminated plate can be modeled as an assemblage of beam-plates, i.e. plates of constant width undergoing cylindrical deformation in the  $XZ$ -plane. Accordingly, all the following calculations will be referred to a plate with unit width ( $B = 1$ ).

The proposed model considers four regions partly connected by a distribution of normal and tangential springs, whose elastic constants are  $k_z$  and  $k_x$  (Fig. 3):

- a) the *delaminated film*  $\Omega_d$  of thickness  $H_d < H_b / 2$ , included between the delamination and the nearest external surface;
- b) the *adhering film*  $\Omega_{dk}$  of thickness  $H_d$ , connected to the substrate by the elastic interface;
- c) the *delaminated substrate*  $\Omega_s$  of thickness  $H_s = H_b - H_d$ , included between the delamination and the farthest external surface;
- d) the *adhering substrate*  $\Omega_{sk}$  of thickness  $H_s$ , connected to the film by the elastic interface.

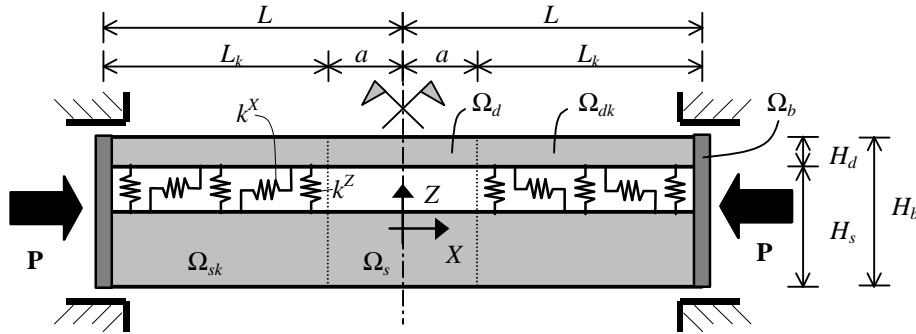


Figure 3 – The Elastic-Interface Model.

**Equilibrium equations.** Only a half plate is considered in the calculation scheme, where suitable restraints on the symmetry axis and clamped end conditions are assumed (Fig. 4). An auxiliary reference system with the origin at the delamination front, such that  $X_k = X - a$ , is also fixed.

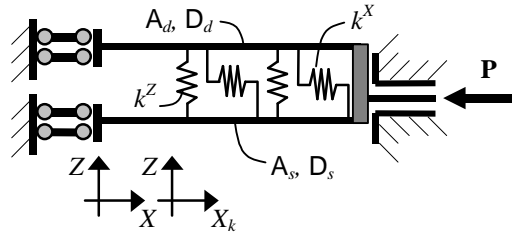


Figure 4 – EI Model: calculation scheme.

Each sublaminates is modeled as beam-plate undergoing moderate rotations. Let  $A_d = E_X H_d$  and  $D_d = E_X H_d^3 / 12$  be the extensional and bending stiffnesses of the film, respectively; let  $A_s = E_X H_s$  and  $D_s = E_X H_s^3 / 12$  be those of the substrate; let  $A_b = E_X H_b$  and  $D_b = E_X H_b^3 / 12$  be those of the base laminate. According to von Kármán's theory, the following differential equation

$$\begin{aligned} \frac{\partial^4 w}{\partial X^4} + 2 \frac{\partial^4 w}{\partial X^2 \partial Y^2} + \frac{\partial^4 w}{\partial Y^4} = \\ = \frac{1}{D} \left( N^X \frac{\partial^2 w}{\partial X^2} + 2N^{XY} \frac{\partial^2 w}{\partial X \partial Y} + N^Y \frac{\partial^2 w}{\partial Y^2} + \frac{\partial m^X}{\partial X} + \frac{\partial m^Y}{\partial Y} - f^X \frac{\partial w}{\partial X} - f^Y \frac{\partial w}{\partial Y} + q \right) \end{aligned} \quad (1)$$

governs the bending problem for each sublaminates; while the extensional problem is described by

$$\frac{\partial N^X}{\partial X} + \frac{\partial N^{XY}}{\partial Y} + f^X = 0 \quad \text{and} \quad \frac{\partial N^{XY}}{\partial X} + \frac{\partial N^Y}{\partial Y} + f^Y = 0, \quad (2)$$

where, as usual,  $w$  is the transverse displacement;  $m^X$  and  $m^Y$  are the distributed moment loads;  $f^X$ ,  $f^Y$  and  $q$  are the distributed loads and, finally,  $N^X$ ,  $N^{XY}$ , and  $N^Y$  are the membrane forces.

In the present model, all the derivatives w.r.t.  $Y$  and all the quantities in the  $Y$ -direction are zero. The load terms  $q$  and  $f^X$  are zero for the delaminated regions,  $\Omega_d$  and  $\Omega_s$ , while they are equal to the elastic reactions of the interface for the adhering sublaminates,  $\Omega_{dk}$  and  $\Omega_{sk}$ .

It is convenient to define the constants  $\lambda$ ,  $\mu$  and  $\omega$ , all having the dimensions of length:

$$\lambda^2 = \frac{D_d}{P_d^C} = -\frac{D_d}{N_d^X}, \quad (3)$$

$$\mu^4 = 4 \frac{D_d}{k_Z}, \quad (4)$$

$$\omega^2 = \frac{1}{k_X} \frac{1}{1/A_d + 1/A_s}, \quad (5)$$

where  $P_d^C = -N_d^X$  is the *buckling load of the delaminated region*, to be determined as explained in the following. The load that correspondingly is applied to the base laminate is  $P^C = P_d^C (A_b / A_d)$ .

According to the so-called “thick column” hypothesis, it is here supposed that  $D_s \gg D_d$ . So, any transverse displacements of the substrate,  $w_s$  and  $w_{sk}$ , are neglected, while the transverse displacements of the film,  $w_d$  and  $w_{dk}$ , are taken into account. Axial displacements,  $u_d$ ,  $u_{dk}$ ,  $u_s$ , and  $u_{sk}$ , are considered in all sublaminates. With this, and by using the constitutive law to express axial forces in terms of displacements, the governing equations become:

$$\frac{\partial^4 w_d}{\partial X^4} + \frac{1}{\lambda^2} \frac{\partial^2 w_d}{\partial X^2} = 0, \quad (6)$$

$$\frac{\partial u_d}{\partial X} + \frac{1}{2} \left( \frac{\partial w_d}{\partial X} \right)^2 + \frac{P_d^C}{A_d} = 0, \quad (7)$$

for the delaminated film  $\Omega_d$ ;

$$\frac{\partial^4 w_{dk}}{\partial X_k^4} - \frac{A_d}{D_d} \frac{\partial}{\partial X_k} \left\{ \left[ \frac{\partial u_{dk}}{\partial X_k} + \frac{1}{2} \left( \frac{\partial w_{dk}}{\partial X_k} \right)^2 \right] \frac{\partial w_{dk}}{\partial X_k} \right\} + \frac{4}{\mu^4} w_{dk} = 0, \quad (8)$$

$$\frac{\partial^2 u_{dk}}{\partial X_k^2} + \frac{1}{2} \frac{\partial}{\partial X_k} \left( \frac{\partial w_{dk}}{\partial X_k} \right)^2 - \frac{1}{\omega^2} \frac{1}{1 + A_d/A_s} (u_{dk} - u_{sk}) = 0, \quad (9)$$

for the adhering film  $\Omega_{dk}$ ;

$$w_s = 0, \quad (10)$$

$$\frac{\partial u_s}{\partial X} + \frac{P - P_d^C}{A_s} = 0, \quad (11)$$

for the delaminated substrate  $\Omega_s$ ;

$$w_{sk} = 0, \quad (12)$$

$$\frac{\partial^2 u_{sk}}{\partial X_k^2} + \frac{1}{\omega^2} \frac{1}{1 + A_s/A_d} (u_{dk} - u_{sk}) = 0, \quad (13)$$

for the adhering substrate  $\Omega_{sk}$ .

### Solution of the problem

**Equilibrium in the post-critical phase.** An exact explicit solution to the above stated differential problem could be obtained in the simpler case with no tangential springs ( $k_X = 0$ ), leading to what is called here the *Winkler-Interface Model*. Despite the choice of not considering any tangential stresses is questionable in principle, the derivation of an exact solution is useful to test the results of other approximate analyses [21,22]. The final expressions that were obtained are rather lengthy and cannot be given here, but results in the shape of graphs are reported in the following section.

In the more realistic, general case ( $k_Z \neq 0$  and  $k_X \neq 0$ ) of the *Elastic-Interface Model*, an approximate explicit solution was found, by neglecting the nonlinear contribution to the axial strain in Eqns. (8) and (9). Consequently, the adhering film  $\Omega_{dk}$  is treated as a standard beam-plate that undergoes transverse displacements, acting as an elastic restraint for the delaminated film  $\Omega_d$ , but does not take part directly in the instability phenomenon.

The final expressions of the transverse displacements of the film in the post-critical phase are

$$w_d = A_d \left( \cos \frac{X}{\lambda} + d_d \right), \quad (14)$$

$$w_{dk} = A_d \left[ \left( a_{dk} \cosh \frac{X_k}{\mu} + b_{dk} \sinh \frac{X_k}{\mu} \right) \cos \frac{X_k}{\mu} + \left( c_{dk} \cosh \frac{X_k}{\mu} + d_{dk} \sinh \frac{X_k}{\mu} \right) \sin \frac{X_k}{\mu} \right], \quad (15)$$

where  $d_d$ ,  $a_{dk}$ ,  $b_{dk}$ ,  $c_{dk}$ , and  $d_{dk}$  are dimensionless constants of integration and  $A_d$ , with the dimensions of length, is the amplitude of the sinusoid representing the transverse displacement of  $\Omega_d$ .

The expressions of the axial displacements are

$$u_d = -\frac{P^C}{A_b} X - \frac{A_d^2}{8\lambda} \left( \frac{2X}{\lambda} - \sin \frac{2X}{\lambda} \right), \quad (16)$$

$$u_{dk} = -\frac{P}{A_b} (X_k + a) + \frac{P - P^C}{A_b} \left( a \cosh \frac{X_k}{\omega} + \omega \sinh \frac{X_k}{\omega} \right) - \frac{A_d^2}{8\lambda} \left( \frac{2a}{\lambda} - \sin \frac{2a}{\lambda} \right) \left( \frac{A_s}{A_b} \cosh \frac{X_k}{\omega} + \frac{A_d}{A_b} \right), \quad (17)$$

$$u_s = -\frac{1}{A_s} \left( P - \frac{A_d}{A_b} P^C \right) X, \quad (18)$$

$$u_{sk} = -\frac{P}{A_b} (X_k + a) - \frac{A_d}{A_b} \left[ \frac{P - P^C}{A_s} \left( a \cosh \frac{X_k}{\omega} + \omega \sinh \frac{X_k}{\omega} \right) - \frac{A_d^2}{8\lambda} \left( \frac{2a}{\lambda} - \sin \frac{2a}{\lambda} \right) \left( \cosh \frac{X_k}{\omega} - 1 \right) \right]. \quad (19)$$

By putting expressions (14) to (19) into the boundary conditions (whose expressions are here omitted for brevity), a set of linear homogeneous algebraic equations for the six unknown constants of integration is obtained. For a nontrivial solution to exist, its determinant,

$$\det \mathbf{R} = -\frac{2}{\lambda^3 \mu^5} \sec^2 \frac{L_k}{\mu} \left\{ 2\lambda \mu \left( \operatorname{sech}^2 \frac{L_k}{\mu} \sin \frac{L_k}{\mu} \cos \frac{L_k}{\mu} + \tanh \frac{L_k}{\mu} \right) \cos \frac{a}{\lambda} + \left[ (2\lambda^2 + \mu^2) \operatorname{sech}^2 \frac{L_k}{\mu} \cos^2 \frac{L_k}{\mu} + 2\lambda^2 - \mu^2 \right] \sin \frac{a}{\lambda} \right\}, \quad (20)$$

must vanish. Hence, the buckling load of the delaminated region,  $P_d^C = D_d / \lambda^2$ , can be found by solving numerically Eqn. (20).

The nondimensional constants of integration are determined as

$$d_d = \left( \frac{\mu^2}{2\lambda^2} \tanh \frac{L_k}{\mu} \tan \frac{L_k}{\mu} - 1 \right) \cos \frac{a}{\lambda} + \frac{\mu}{4\lambda^3} \left[ (2\lambda^2 + \mu^2) \tanh \frac{L_k}{\mu} + (2\lambda^2 - \mu^2) \tan \frac{L_k}{\mu} \right] \sin \frac{a}{\lambda} \quad (21)$$

$$a_{dk} = \frac{\mu^2}{2\lambda^2} \tanh \frac{L_k}{\mu} \tan \frac{L_k}{\mu} \cos \frac{a}{\lambda} + \frac{\mu}{4\lambda^3} \left[ (2\lambda^2 + \mu^2) \tanh \frac{L_k}{\mu} + (2\lambda^2 - \mu^2) \tan \frac{L_k}{\mu} \right] \sin \frac{a}{\lambda} \quad (22)$$

$$b_{dk} = -\frac{\mu(2\lambda^2 + \mu^2)}{4\lambda^3} \sin \frac{a}{\lambda}, \quad (23)$$

$$c_{dk} = -\frac{\mu(2\lambda^2 - \mu^2)}{4\lambda^3} \sin \frac{a}{\lambda}, \quad (24)$$

$$d_{dk} = -\frac{\mu^2}{2\lambda^2} \cos \frac{a}{\lambda}. \quad (25)$$

The amplitude  $A_d$ , which is zero throughout the pre-critical phase, increases after buckling has occurred, according to the following law

$$A_d^2 = \frac{8\lambda}{2a/\lambda - \sin(2a/\lambda)} \left( a + \omega \tanh \frac{L_k}{\omega} \right) \frac{P - P^C}{A_s} L, \quad (26)$$

derived by enforcing compatibility between the axial displacements of the film and of the substrate.

**Delamination growth.** All the relevant quantities, such as resultant forces and moments, stresses and strains, displacements, etc. can now be determined explicitly in terms of the post-critical solution. In particular, the normal and tangential interlaminar stresses, whose knowledge is necessary in view of the application of a mixed-mode crack-growth criterion, are

$$\sigma_{zz} = k_z A_d \left[ \left( a_{dk} \cosh \frac{X_k}{\mu} + b_{dk} \sinh \frac{X_k}{\mu} \right) \cos \frac{X_k}{\mu} + \left( c_{dk} \cosh \frac{X_k}{\mu} + d_{dk} \sinh \frac{X_k}{\mu} \right) \sin \frac{X_k}{\mu} \right], \quad (27)$$

$$\tau_{zx} = -k_x \frac{P - P^C}{A_s} \omega \left( \tanh \frac{L_k}{\omega} \cosh \frac{X_k}{\omega} - \sinh \frac{X_k}{\omega} \right). \quad (28)$$

By the virtual crack closure technique, the energy release rate,  $G = -\partial\Pi / \partial a$  ( $\Pi$  being the total potential energy of the system), is split into the sum of the contributions of modes I and II,

$$G_I = \lim_{\Delta a \rightarrow 0} \frac{1}{2\Delta a} \int_0^{\Delta a} \Delta \hat{w}(\bar{X}_k - \Delta a) \sigma_{zz}^*(X_k) dX_k, \quad (29)$$

$$G_{II} = \lim_{\Delta a \rightarrow 0} \frac{1}{2\Delta a} \int_0^{\Delta a} \Delta \hat{u}(\bar{X}_k - \Delta a) \tau_{zx}^*(X_k) dX_k, \quad (30)$$

where the hat (^) refers to a plate where the delamination has virtually grown by a length  $\Delta a$  and the star (\*) is relative to the effective system. By substituting the previously obtained solution into (29) and (30), by performing the integration and the limit, the following expressions are finally found:

$$G_I = \frac{1}{2} k_z a_{dk}^2 \frac{8\lambda}{2a/\lambda - \sin(2a/\lambda)} \left( a + \omega \tanh \frac{L_k}{\omega} \right) \frac{P - P^C}{A_s}, \quad (31)$$

$$G_{II} = \frac{1}{2} k_x \left( \omega \tanh \frac{L_k}{\omega} \frac{P - P^C}{A_s} \right)^2. \quad (32)$$

**Some results**

As an application, a plate with  $L = 100$  mm,  $H_d = 1$  mm and  $H_b = 10$  mm is considered. The assumed elastic moduli are typical of a fiber-reinforced composite:  $E_X = 113000$  MPa,  $E_Y = 9000$  MPa,  $G_{XY} = 3820$  MPa. In the following graphs, load values are made nondimensional by dividing them by the Euler load,  $P^{EUL} = \pi^2 D_b / L^2 = 9294$  N/mm (which is the buckling load of the undamaged plate) and the delamination length,  $a$ , is divided by the plate length,  $L$ .

The curves plotted in Figs. 5 and 6, computed using the *WI* and the *EI Models*, respectively, represent the buckling load of the plate,  $P^C$ , as a function of the delamination length,  $a$ , for a range of values of the normal spring constant,  $k_z$ .

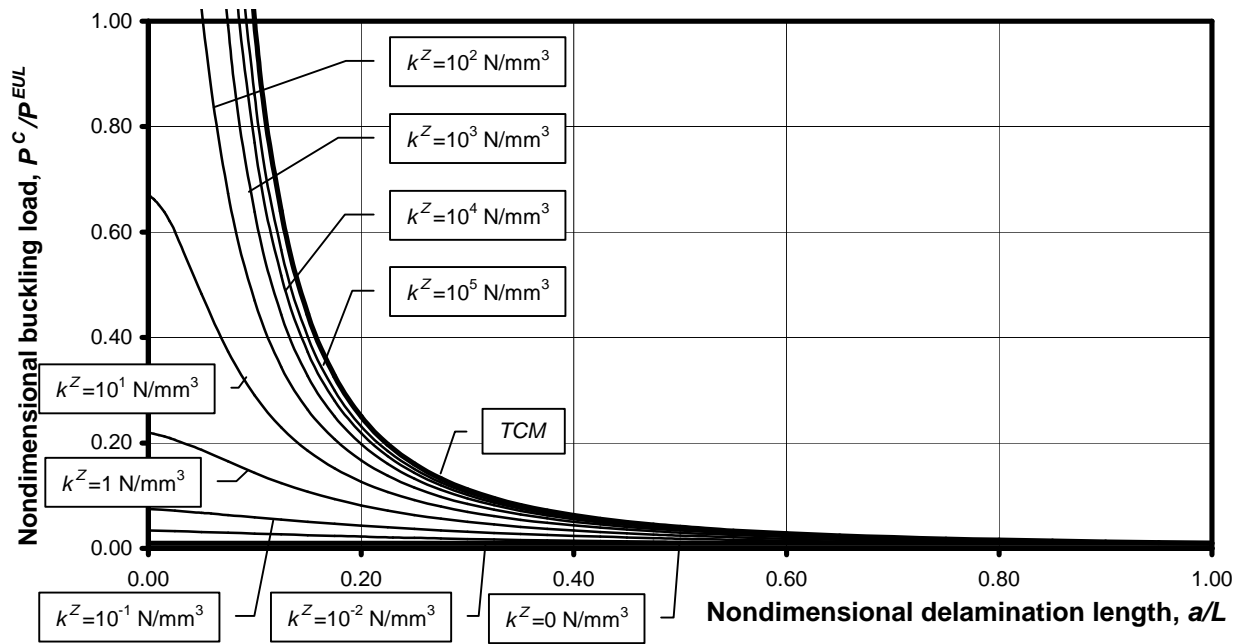


Figure 5 – *WI Model*: Buckling load of the plate vs. delamination length.

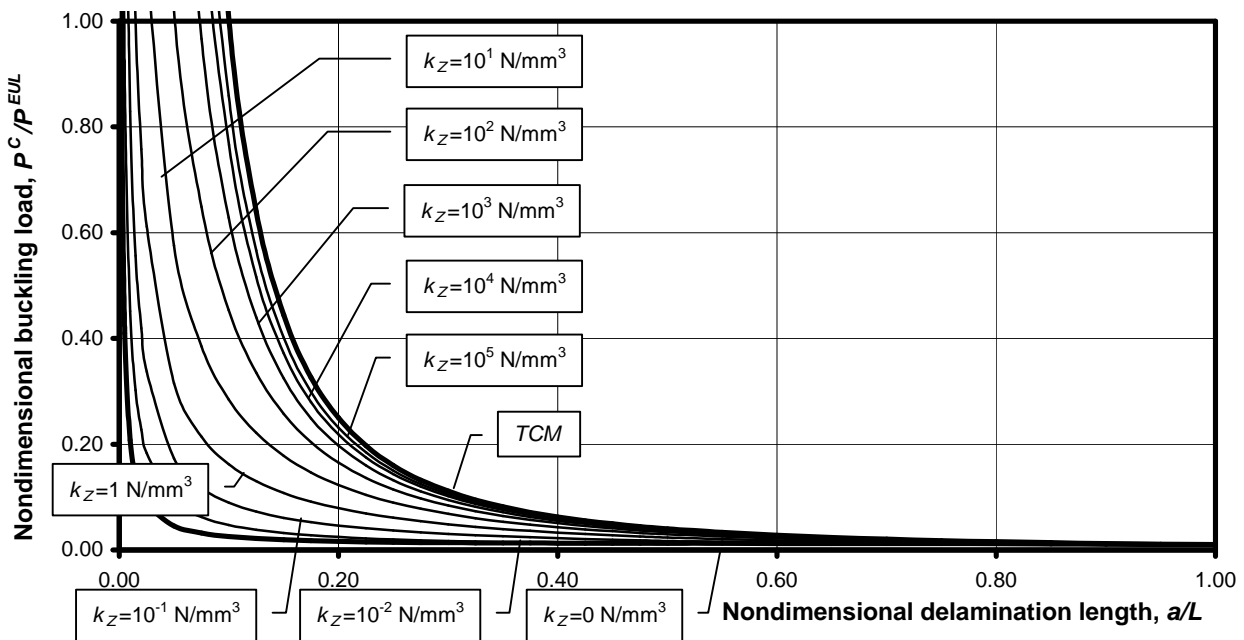


Figure 6 – *EI Model*: Buckling load of the plate vs. delamination length.

In both cases,  $P^C$  is a decreasing functions of  $a$ , and as  $a/L \rightarrow 1$  (complete delamination),  $P^C$  goes to  $P^{C0} = (A_b / A_d) \pi^2 D_d / L^2$ . As  $a/L \rightarrow 0$  (no delamination), the *WI Model* furnishes finite values, namely the buckling loads of a beam on an elastic foundation. Instead, the *EI Model* predicts loads that go to infinity. This is a consequence of having neglected the instability of the adhering film. In any case, values of  $P^C/P^{EUL} > 1$  have no physical meaning and must therefore be excluded.

As  $k_z \rightarrow \infty$  (rigid interface), the buckling loads furnished by both models approach those of the *TC Model*. Instead, as  $k_z \rightarrow 0$  (no interface),  $P^C \rightarrow P^{C0}$ .

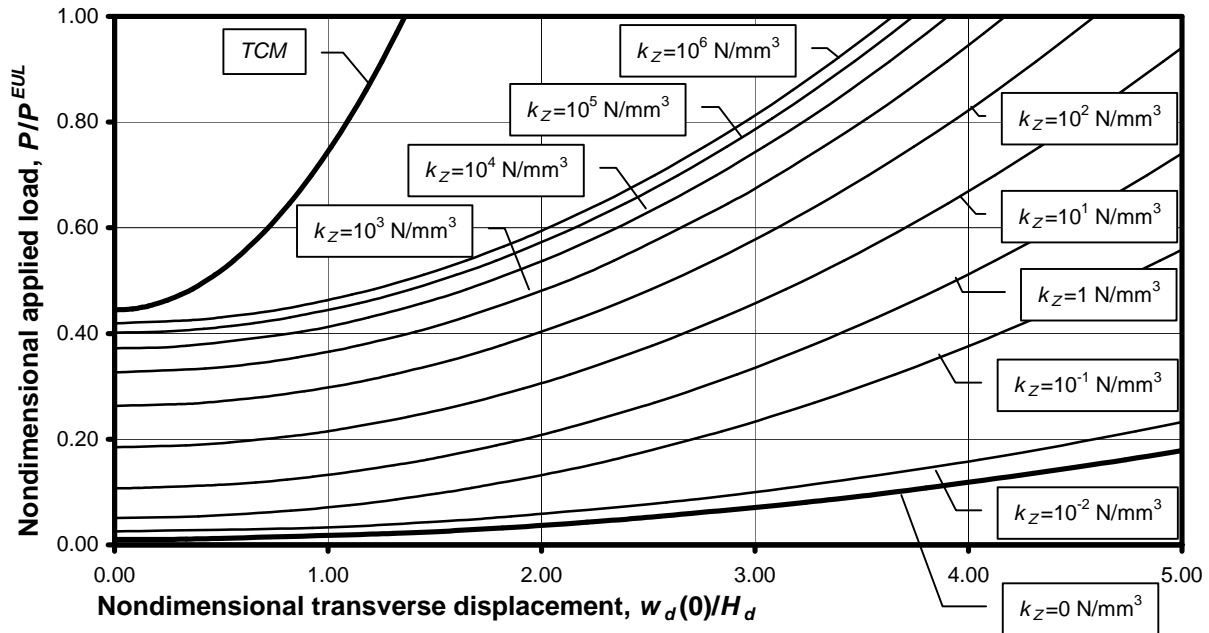


Figure 7 – *WI Model*: Applied load vs. transverse displacement of the midpoint.

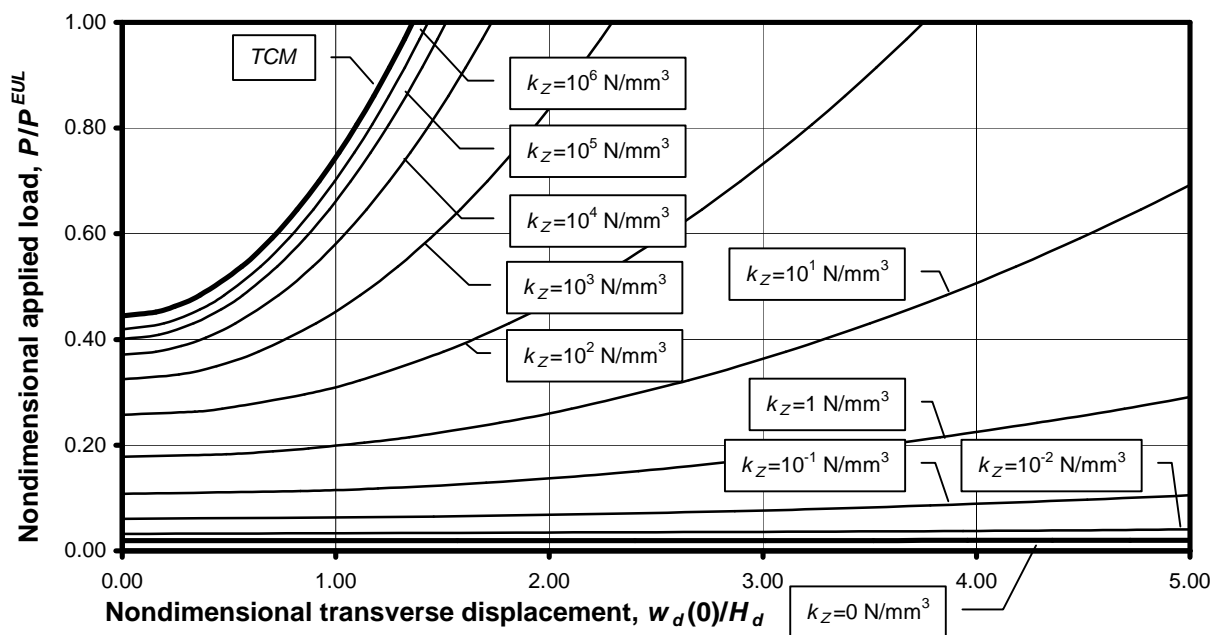


Figure 8 – *EI Model*: Applied load vs. transverse displacement of the midpoint.

In a composite laminate, the interface represents the thin layer of resin between the laminae, so its elastic constants should be assigned in terms of the properties of the resin itself [26]. Lacking those data, their values are commonly deduced from the properties of a single lamina, as follows:

$$k_z = \frac{E_Y}{t}, \quad \text{and} \quad k_x = \frac{G_{XY}}{t}, \quad (33)$$

where  $E_Y$  and  $G_{XY}$  are the elasticity moduli in the direction orthogonal to fibers and  $t$  is the thickness of the lamina [19,20]. For a typical fiber-reinforced composite, it can be approximately expected that  $k_z = 10^4 \div 10^6 \text{ N/mm}^3$  and  $k_x = 1/5 \div 1/2 k_z$ . So, as regards the buckling load, the *WI* and the *EI Models* can be utilized indifferently, since their predictions nearly coincide for  $k_z \geq 10^2 \text{ N/mm}^3$ .

Moving on to examine the post-critical behavior, a fixed delamination length,  $a = 15 \text{ mm}$ , and a tangential spring constant  $k_x = k_z / 2$  are assumed. Figs. 7 and 8, obtained via the *WI* and the *EI Models*, respectively, show the applied load vs. the transverse displacement of the midpoint of the delaminated region,  $w_d(0)$ , made nondimensional by dividing it by  $H_d$ . The *WI Model* reveals a less stiff response than the *EI Model*, due to the lack of a tangential interlaminar bonding. It is worth noting how, as  $k_z \rightarrow \infty$ , the *WI Model* does *not* converge to the *TC Model*, while the *EI Model* does.

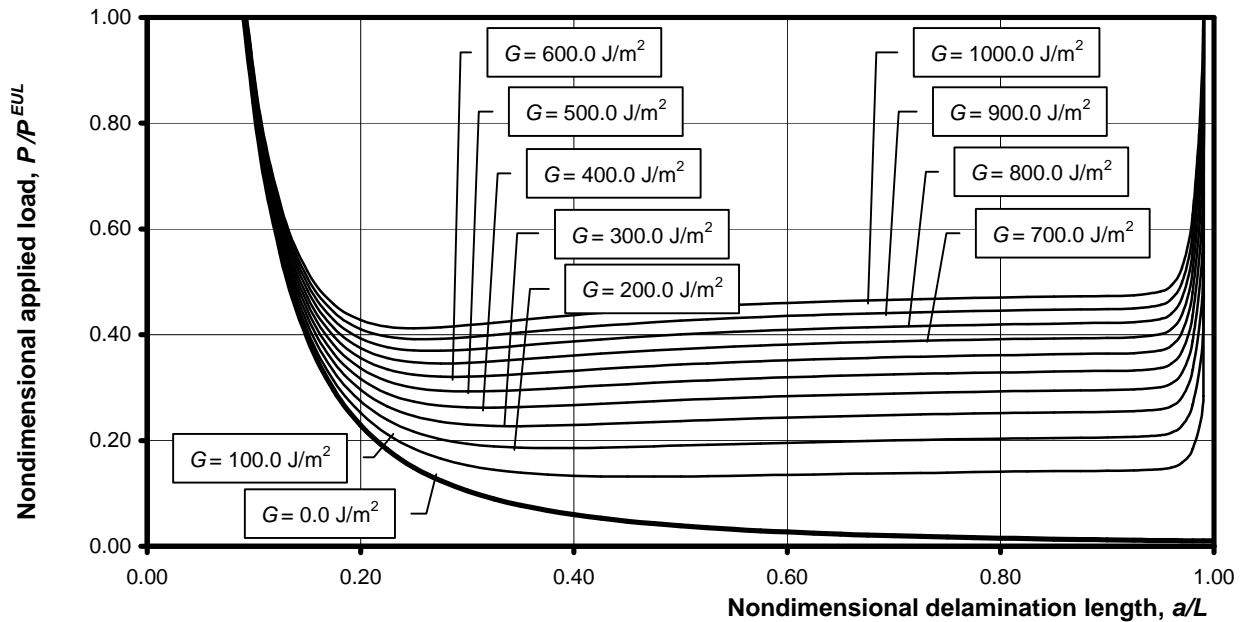


Figure 9 – *EI Model*: Energy Release Rate vs. delamination length and applied load.

Finally, the process of delamination growth for the *EI Model* is considered, assuming the elastic constants,  $k_z = 5.6 \times 10^4 \text{ N/mm}^3$  and  $k_x = 2.4 \times 10^4 \text{ N/mm}^3$ , given by Eqns. (33) with  $t = 0.16 \text{ mm}$ . According to Griffith's criterion, the crack starts to grow when the energy release rate,  $G$ , attains a critical value,  $G^C$ . Fig. 9 represents a contour plot of  $G$  as a function of the nondimensional delamination length,  $a/L$ , and applied load,  $P/P^{EUL}$ . During the pre-critical phase, the film and the substrate do not undergo any relative displacements, thus the interlaminar stresses are zero and so is  $G$ . Consequently, no growth is predicted for loads less than the buckling load. During the post-critical phase,  $G$  increases with increasing load. When the critical value is reached, delamination growth occurs and the point representative of the state of the system,  $(a, P)$ , moves along a contour line,  $G = G^C$ . Growth will be stable if  $P$  increases with increasing  $a$ , unstable if  $P$  decreases.

The critical energy release rate,  $G^C$ , is a material constant to be determined by experiments. Nevertheless, for composite laminates, values measured in a pure mode-II test,  $G_{II}^C$ , can be several times those measured in a pure mode-I test,  $G_I^C$ . So, a more realistic crack-growth criterion should account for the *mode mixity*, by assigning different weights to the contributions of modes I and II [18]. A rough choice, yet useful for the sake of illustration, is assuming that only one mode is relevant and that the delamination grows when either  $G_I = G_I^C$  or  $G_{II} = G_{II}^C$ . Fig. 10 and 11 represent

the contour plots of the mode-I and mode-II energy release rates,  $G_I$  and  $G_{II}$ , respectively.  $G_I$ -contour lines are initially decreasing with  $a$ , then they attain a minimum and afterwards they become increasing curves. Consequently, the mode-I criterion predicts stable growth for delamination lengths greater than a certain value. On the contrary,  $G_{II}$ -contour lines are decreasing curves, corresponding to unstable growth, nearly to  $a = L$  (complete delamination).

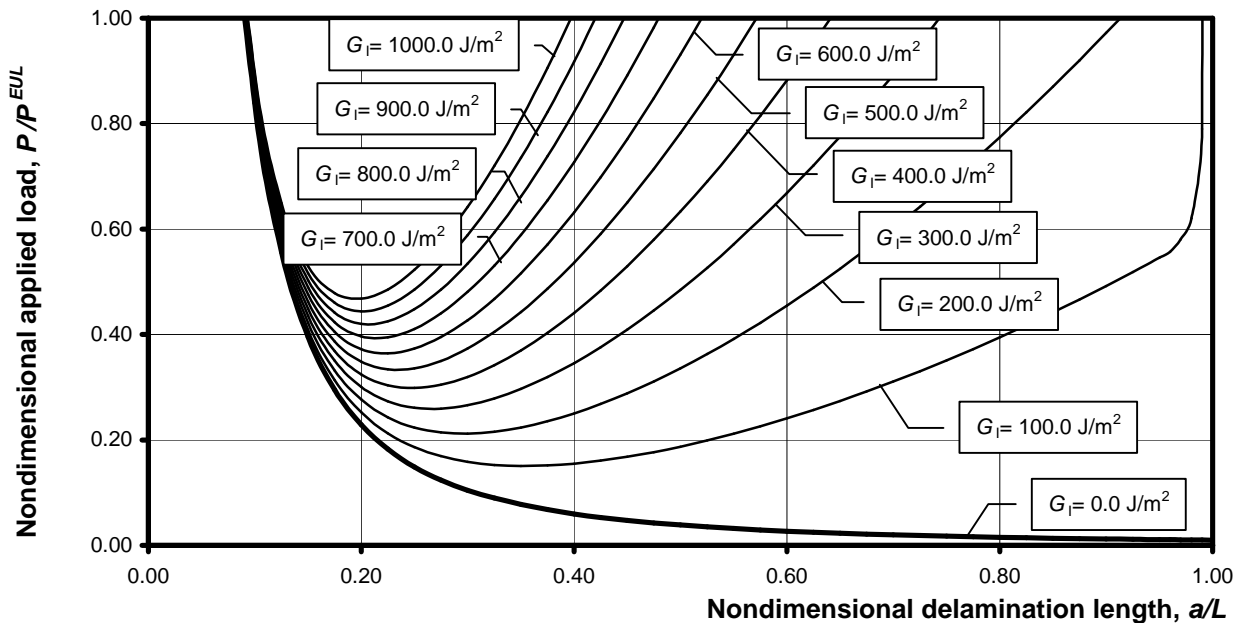


Figure 10 – EI Model: Mode-I (opening) Energy Release Rate vs. delamination length and applied load.

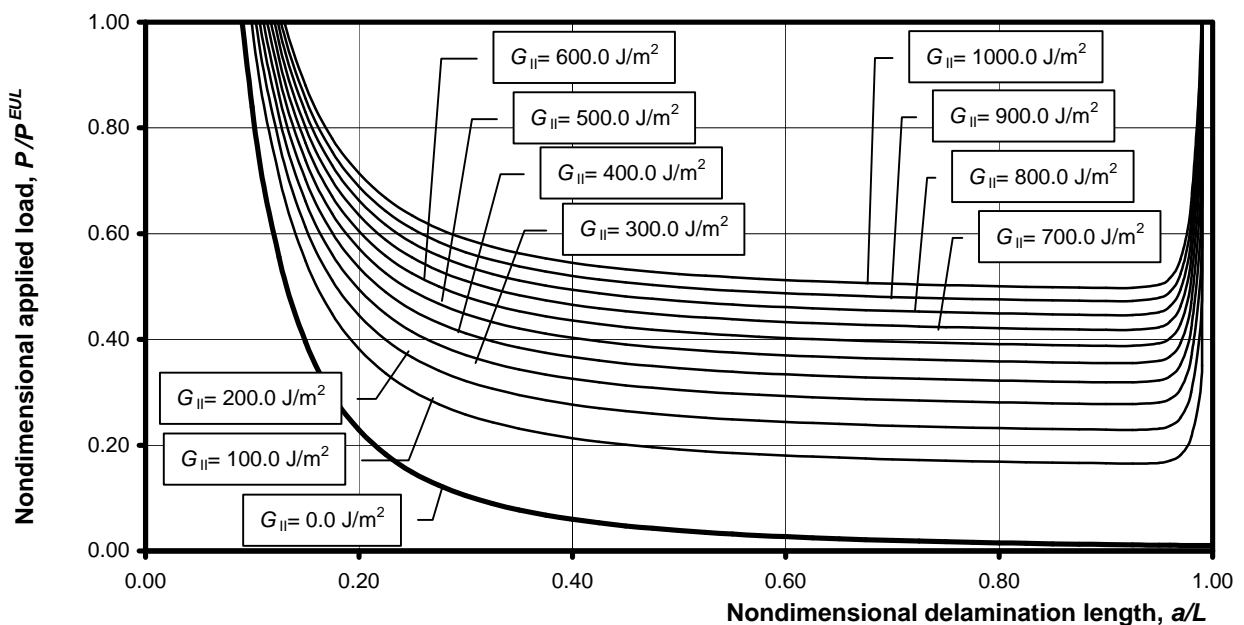


Figure 11 – EI Model: Mode-II (sliding) Energy Release Rate vs. delamination length and applied load.

### Conclusions

A one-dimensional model of a delaminated plate with an elastic interface between sublaminates was presented. The governing equations were solved explicitly in two cases, leading to a simpler *Winkler-Interface Model* and to a more complex *Elastic-Interface Model*. The virtual crack closure technique was used to deduce the expressions of the mode-I and mode-II energy release rates.

Numerical results illustrated the role played by the geometric and elastic parameters of the models. For values corresponding to real laminates, the *WI* and the *EI Models* furnished nearly the same buckling loads (lower than those given by the *Thick Column Model*). In the post-critical phase, the *WI Model* showed a less stiff response than the *EI Model*. In the limit case of a rigid interface, the *WI Model* did not converge to the *TC Model*, while the *EI Model* did. These circumstances should warn against the errors that can be made, by neglecting the tangential interlaminar stresses.

Finally, the process of delamination growth was briefly discussed. The contour plots of  $G$ ,  $G_I$  and  $G_{II}$  revealed markedly different qualitative trends, so that different predictions about crack growth and its stability were possible, depending on which mode had a prevailing weight in the adopted growth criterion. The taking into account of the mode mixity is thus confirmed as a crucial issue.

## References

- [1] L.M. Kachanov: *Polymer Mech.* Vol. 12 (1977), pp. 812ff.
- [2] H. Chai, C.D. Babcock and W.G. Knauss: *Int. J. Solids Struct.* Vol. 17 (1981), pp. 1069ff.
- [3] J.D. Whitcomb: *J. Compos. Materials* Vol. 15 (1981), pp. 403ff.
- [4] W.J. Bottega and A. Maewal: *ASME J. Appl. Mech.* Vol. 50 (1983), pp. 184ff.
- [5] W.-L. Yin: *Int. J. Solids Struct.* Vol. 21 (1985), pp. 503ff.
- [6] X. Zhang and S. Yu: *Int. J. Solids Struct.* Vol. 36 (1999), pp. 1799ff.
- [7] O. Allix and A. Corigliano: *Int. J. Solids Struct.* Vol. 36 (1999), pp. 2189ff.
- [8] R. Massabò and B.N. Cox: *J. Mech. Phys. Solids* Vol. 47 (1999), pp. 1265ff.
- [9] J.W. Hutchinson, M.Y. He and A.G. Evans: *J. Mech. Phys. Solids* Vol. 48 (2000), pp. 709ff.
- [10] D. Bruno and F. Greco: *Int. J. Solids Struct.* Vol. 37 (2000), pp. 6239ff.
- [11] F. Lachaud, B. Lorrain, L. Michel and R. Barriol: *Comp. Sci. Tech.* Vol. 58 (1998), pp. 727ff.
- [12] P.D. Panagiotopoulos and G.E. Stavroulakis: *J. Elasticity* Vol. 23 (1990), pp. 69ff.
- [13] E. Madenci: *Int. J. Sol. Struct.* Vol. 27 (1991), pp. 1773ff.
- [14] B. Storåkers and B. Andersson: *J. Mech. Phys. Solids* Vol. 36 (1988), pp. 689ff.
- [15] J.W. Hutchinson and Z. Suo: *Adv. Appl. Mech.* Vol. 29 (1992), pp. 63ff.
- [16] W.T. Chow and S.N. Atluri: *Comput. Mech.* Vol. 21 (1998), pp. 1ff.
- [17] I. Sheinman and G.A. Kardomateas: *Int. J. Solids Struct.* Vol. 34 (1997), pp. 451ff.
- [18] C. Hwu, C.J. Kao and L.E. Chang: *J. Compos. Mat.* Vol. 29 (1995), pp. 1962ff.
- [19] O. Allix, and P. Ladevèze: *Compos. Struct.* Vol. 22 (1992), pp. 235ff.
- [20] A. Corigliano: *Int. J. Solids Struct.* Vol. 30 (1993), pp. 2779ff.
- [21] A.J. Vizzini and P.A. Lagace: *J. Compos. Mat.* Vol. 21 (1987), pp. 1106ff.
- [22] D. Bruno and A. Grimaldi: *Int. J. Solids Struct.* Vol. 26 (1990), pp. 313ff.
- [23] N. Point and E. Sacco: *Int. J. Solids Struct.* Vol. 33 (1996), pp. 483ff.
- [24] F. Fraternali: *Theor. Appl. Fracture Mech.* Vol. 25 (1996), pp. 225ff.
- [25] S.-H. Cheng, C.-C. Lin and J.T.-S. Wang: *Int. J. Solids Struct.* Vol. 34 (1997), pp. 275ff.
- [26] M. Oriunno, A. Frediani and A. Lazzeri: *Engng. Fracture Mech.* Vol. 55 (1996), pp. 1001ff.